Nonlinear Modal Decoupling Based Power System Transient Stability Analysis

Bin Wang, *Member, IEEE*, Kai Sun, *Senior Member, IEEE*, and Xin Xu, *Student Member, IEEE*

***Abstract*—Nonlinear modal decoupling (NMD) was recently proposed to nonlinearly transform a multi-oscillator system into as many decoupled oscillators as the oscillation modes of interests with the original system. Those decoupled oscillators together provide a fairly accurate approximation of behaviors of the original system in an extended neighborhood of the equilibrium. Each oscillator has just one degree of freedom and hence can easily be analyzed to infer the nonlinear dynamics of the original system associated with one oscillation mode. As the first attempt of applying the NMD methodology to realistic power system models, this paper proposes an NMD-based approach for the early warning of the oscillation mode that may most likely develop into a mode of transient instability. For a multi-machine power system, the approach first derives decoupled nonlinear oscillators by a coordinates transformation, and then applies Lyapunov stability analysis to decoupled oscillators to assess the stability of the original system. For large-scale power grids, the proposed approach can be efficiently applied by conducting NMD regarding only selected modes. Case studies on a 3-machine 9-bus system and a Northeast Power Coordinating Council (NPCC) 48-machine 140-bus system show the potentials of the approach in early warning of transient instability for multi-machine systems.**

***Index Terms*—Nonlinear modal decoupling, transient stability analysis, energy function, first-integral, Zubov's method.**

I. Introduction

MODERN power systems are sometime operated close to their stability limits. Care must be taken in the operation to avoid driving the system to cross any limit, or catastrophic consequences like wide-scale power outages and blackouts may occur. In reality, the instability is often developed from certain oscillation modes. For instance, before the occurrence of the August 10, 1996 Western Interconnection Blackout, poorly-damped oscillations at around 0.26Hz were observed which later developed into an instability leading to an uncontrolled outage and interrupting the electric service to more than 7 million customers [1]. Similar for the August 14, 2003 Blackout, due to a lack of adequate real-time situational awareness, many power oscillation events were observed but no symptoms of instability were captured [2].

To this end, many tools have been proposed to signal an early warning of instability and provide mitigation strategies to the system operator. Numerical time-domain simulation on "what-if" scenarios is a widely-adopted approach by power industry for identification of potential transient instabilities, whose results are accurate but contingency-dependent. Applying this time-consuming simulation-based approach to provide an early warning of transient instability in real time is very challenging especially for large-scale modern power systems due to the computational burden. Many high-performance computing approaches have been proposed to speed up the simulation, but currently they are still not ready for control rooms [3]. Hybrid approaches using both PMU measurements and the system dynamical model provide an alternative framework, which uses PMUs to online monitor system dynamics and generate an early warning signal based on the information gathered online or prepared offline [4]-[8]. In addition, eigen-components calculated from the linearized dynamical model was used to identify the potential source of instability in real time in [9]. The critical cutset separating the system into two oscillating groups, usually about a certain oscillation mode, was developed to identify the upcoming transient instability in the online environment [10].

The recently proposed nonlinear modal decoupling (NMD) [11] shows promising results in analyzing large disturbances, e.g. approximating the closest unstable equilibrium points [12] and estimating the boundary of transient stability region [13]. The NMD methodology was inspired by the normal form theory [14]-[16] which employs a series of nonlinear coordinates transformations toward formal linearization of a nonlinear system up to a desired order in an extended neighborhood of the equilibrium. Unlike the normal form method, the NMD finds nonlinear coordinates transformations to only eliminate coupling terms among different modes. Thus, the resulting transformed system is still nonlinear but has inter-modal coupling eliminated up to a desired order. This paper is the first attempt to apply NMD to the early warning of power system transient instability. NMD can systematically construct as many decoupled nonlinear oscillators as the system's oscillation modes, where each nonlinear oscillator is associated with each oscillation mode. Therefore, the dynamics of the original system subject to large disturbances can be analyzed and visualized with respect to only a few selected critical modes through NMD (note that only very few oscillation modes, e.g. mostly six or less, can be excited in any single contingency even for large-scale power systems [17]). If system operators have some knowledge on which modes the instability may be developed from, they can intentionally monitor the system dynamics on those critical

This work was supported in part by NSF under Grant ECCS-1553863 and in part by the ERC Program of the NSF and DOE under Grant EEC-1041877.

B. Wang, K. Sun and X. Xu are with the University of Tennessee, Knoxville, TN 37996 USA (e-mail:bwang13@vols.utk.edu, kaisun@utk.edu, xxu30@vols.utk.edu).

modes and interfaces and take preventive and prepare remedial control strategies to avoid a potential instability.

The rest of the paper is organized as follows: Section II briefly reviews the NMD method for power systems. Section III presents three methods for estimating the stability boundary of each mode-decoupled system determined by NMD, including a simulation-based method as the benchmark. The application of NMD on early warning of the oscillatory mode that may most likely develop into a transient instability is introduced in Section IV with large power systems considered. Case studies on both two small systems and a large NPCC 48-machine 140-bus system are presented in Section V to validate the proposed approach. Section VI draws conclusions and envision future works.

II. Nonlinear Modal Decoupling of Power Systems

Given a multi-oscillator system described by N ordinary differential equations, which may represent a power system:

$$\dot{\mathbf{x}} = \mathbf{f}(\mathbf{x}) \tag{1}$$

where $\mathbf{x}=[x_1, x_2, \ldots, x_N]^{\mathrm{T}}$ is the state vector with the equilibrium at the origin and $\mathbf{f}(\mathbf{x})=[f_1(\mathbf{x}), f_2(\mathbf{x}), \ldots, f_N(\mathbf{x})]^{\mathrm{T}}$ is a smooth vector field (N is an even number). Assume that the Jacobian matrix of $\mathbf{f}(\mathbf{x})$, denoted by A, has $N/2$ conjugate pairs of complex eigenvalues $\lambda_1, \lambda_2, \ldots, \lambda_N$. Without loss of generosity, let λ_{2i-1} and λ_{2i} be a conjugate pair defining the mode i.

It has been shown in [11] that, if the resonance does not happen, the system in (1) can always be transformed to a dynamical system as shown in (2) through a linear transformation that diagonalizes A using its modal matrix (consisting of all right eigenvectors) and a series of homogeneous polynomial transformations defined in (3) and (4) with $p=1, 2, \ldots$.

$$\dot{\mathbf{z}}^{(k)} = \mathbf{\Lambda}\cdot\mathbf{z}^{(k)} + \sum_{j=2}^{k}\mathbf{D}_j(\mathbf{z}^{(k)}) + \sum_{j=k+1}^{\infty}\left(\mathbf{D}_j(\mathbf{z}^{(k)}) + \mathbf{C}_j(\mathbf{z}^{(k)})\right) \tag{2}$$

$$\mathbf{z}^{(p)} = \mathbf{H}_{p+1}(\mathbf{z}^{(p+1)}) \overset{\text{def}}{=} \mathbf{z}^{(p+1)} + \begin{bmatrix} \vdots \\ h_{p+1,2i-1}(\mathbf{z}^{(p+1)}) \\ h_{p+1,2i}(\mathbf{z}^{(p+1)}) \\ \vdots \end{bmatrix} \tag{3}$$

$$\begin{cases} h_{p+1,2i-1}(\mathbf{z}^{(p+1)}) = \sum_{\alpha=1}^{N}\cdots\sum_{\gamma=\eta}^{N} h_{p+1,2i-1,\alpha\cdots\eta\gamma}\underbrace{z_{\alpha}^{(p+1)}\cdots z_{\gamma}^{(p+1)}}_{p+1\text{ terms in total}} \\ h_{p+1,2i}(\mathbf{z}^{(p+1)}) = \overline{h}_{p+1,2i-1}(\mathbf{z}^{(p+1)}) \end{cases} \tag{4}$$

If only k terms of (2) are summated, a truncated approximate of (1) is produced. In (2), $\mathbf{z}^{(k)}=[z_1^{(k)}, z_2^{(k)}, \ldots, z_N^{(k)}]^{\mathrm{T}}$ is the state vector of the transformed system having $z_{2i-1}^{(k)}$ and $z_{2i}^{(k)}$ associated with mode i, and $\mathbf{D}_j$ and $\mathbf{C}_j$ are vector fields whose elements are weighted sums of the terms of degree j about $\mathbf{z}^{(k)}$. $\mathbf{D}_j$ only contains intra-modal terms, i.e. monomials only about the state variables associated with mode i, while $\mathbf{C}_j$ only has inter-modal terms, i.e. monomials each about state variables with different modes. $\mathbf{H}_k(\mathbf{z}^{(k)})$ is the k-th transformation used in NMD, $h_k(\mathbf{z}^{(k)})$ is a k-th order homogeneous polynomial in $\mathbf{z}^{(k)}$. The function h with a "bar" in (4) represents the conjugate of the function under it.

Note that h-coefficients in (4) are not unique. Ref. [11] provides two ways to determine a set of h-coefficients: one assumes that each mode-decoupled system is an equivalent SMIB system, which is called "SMIB assumption"; the other one determines h-coefficients under a so-called "smaller transfer assumption", which tries to avoid propagating nonlinearities from low order terms to high order terms. As reported in [11], the "small transfer assumption" generates a set of h-coefficients leading to a more accurate approximation to the original system than the "SMIB assumption", and hence is adopted throughout this paper.

In (2), all modes are decoupled in the terms of up to order k. If we ignore nonlinear terms of orders $\geq k+1$, where modal coupling still remains, a truncated but mode-decoupled system (5) is resulted, where the pair of equations about each individual mode are completely decoupled from the rest ($2N$-2) equations about other modes.

$$\dot{\mathbf{z}}_{\text{jet}}^{(k)} = \mathbf{\Lambda}\cdot\mathbf{z}_{\text{jet}}^{(k)} + \sum_{j=2}^{k}\mathbf{D}_j(\mathbf{z}_{\text{jet}}^{(k)}) \tag{5}$$

Thus, each mode i can be analyzed using only the associated pair of equations, which are expanded as (6).

$$\begin{cases} \dot{z}_{\text{jet},2i-1}^{(k)} = \lambda_{2i-1}z_{\text{jet},2i-1}^{(k)} + \sum_{\alpha=1}^{N}\sum_{\beta=\alpha}^{N}\mu_{2i-1,\alpha\beta}z_{\text{jet},\alpha}^{(k)}z_{\text{jet},\beta}^{(k)} + \cdots + \\ \quad \sum_{\alpha=1}^{N}\cdots\sum_{\rho=\gamma}^{N}\mu_{2i-1,\alpha\cdots\rho}\underbrace{z_{\text{jet},\alpha}^{(k)}\cdots z_{\text{jet},\rho}^{(k)}}_{k\text{ terms in total}} \overset{\text{def}}{=} f_{\text{jet},2i-1}^{(k)}(\mathbf{z}_{\text{jet}}^{(k)}) \\ \dot{z}_{\text{jet},2i}^{(k)} = f_{\text{jet},2i}^{(k)}(\mathbf{z}_{\text{jet}}^{(k)}) = \overline{f}_{\text{jet},2i-1}^{(k)}(\mathbf{z}_{\text{jet}}^{(k)}) \end{cases} \tag{6}$$

Note that the two state variables and all coefficients in (6) are complex-valued. It would be more convenient to analyze its equivalent real-valued system, whose two state variables have physical meanings of, e.g., displacement and velocity. For this purpose, the linear transformation (7) is used to transform (6) into (8) [11].

$$\begin{bmatrix} z_{\text{jet},2i-1}^{(k)} \\ z_{\text{jet},2i}^{(k)} \end{bmatrix} = \begin{bmatrix} \lambda_{2i-1} & \lambda_{2i} \\ 1 & 1 \end{bmatrix}^{-1}\begin{bmatrix} w_{2i-1} \\ w_{2i} \end{bmatrix} \tag{7}$$

$$\begin{cases} \dot{w}_{2i-1} = \upsilon_{i10}w_{2i-1} + \sum_{l=1}^{k}\upsilon_{i0l}w_{2i}^{l} + \sum_{\substack{j\geq 1, l\geq 0 \\ (j,l)\neq(1,0)}}^{j+l\leq k}\upsilon_{ijl}w_{2i-1}^{j}w_{2i}^{l} \\ \dot{w}_{2i} = w_{2i-1} + \sum_{j\geq 0, l\geq 0}^{2\leq j+l\leq k}\nu_{ijl}w_{2i-1}^{j}w_{2i}^{l} \end{cases} \tag{8}$$

Remarks:

- Ref. [11] also reported that by using (8), analysis on dynamics of system (1) regarding the mode of interest when subject large disturbances becomes much simpler and can be fairly accurate. This enables a new NMD-based analytical approach for roughly estimating the boundary of transient stability region. Instead of analyzing the original system (1), the new approach uses a

pair of differential equations from the decoupled real-valued system (8) corresponding to one mode to estimate the stability boundary observed from the two-dimensional state subspace about that mode. The dynamical behaviors of system (1) can also be transformed to the two-dimensional state subspace for an easier visualization and interpretation using the NMD transformations in (2) and (7). The rest of this paper will focus on an application of NMD for early warning of the oscillatory mode that may most likely develop into a transient instability.

- Errors are introduced in two of the steps from (1) to (8): one is the Taylor expansion of (1) that introduces truncation errors, and the other one is the ignoring of terms of orders >k in (2). Note that dynamics governed by high-order terms may be ignored in a neighborhood of the stable equilibrium point (SEP); however, when the system state is moving toward its stability boundary, the system (5) or its equivalent (8), will have increased errors.
- **Selection of decoupling order k**. On one hand, a too large k may result in a too small validity region of NMD transformation [11], which is not desired since a relative large validity region is needed to hopefully cover the stability boundary. On the other hand, a smaller k is not desired, neither, since which will retain less nonlinearities in the transformed systems, leading to larger errors in the results. Another concern is the conservativeness. Our previous work [18] shown that: (i) using Taylor expansion systems of (1) when k=2, 5, 6 or 9, the resulting analysis is prone to over-estimate stability, which might miss some potential cases of instability and hence is undesired for highly reliable grid operations; (ii) when k=3, 4, 7 or 8, the resulting analysis tends to under-estimate stability to the extent decreasing with k; i.e. the greater k, the more accurate the stability analysis. Finally, it should be noted that a larger k always involves more computational burdens. With all these factors considered, it is recommended to select k only from 3 or 4. The third-order Taylor expansion are adopted in this paper for all case studies.

III. Stability Analysis of Mode-Decoupled Systems

This section introduces the identification of the stability boundary of the real-valued mode-decoupled system in (8). A time simulation aided stability boundary search algorithm is introduced to provide a reference result. Then, two analytical approaches based on the Lyapunov stability theory are presented [19]. With a few simplifying assumptions, the first approach, called the first integral method, constructs a unique Lyapunov function and the critical energy is calculated at the unstable equilibrium point (UEP) close to the origin. The second approach, called the Zubov's method, does not require any assumptions in the original definition of the Lyapunov function. However, the closed-form solution is not always achievable. Thus, the approximation by a truncated power series solution is adopted along with a clear definition of critical energy. It should be noted that other methods, e.g. Popov's method, can also be adopted, which will be investigated in future.

A. Time simulation aided stability boundary search

Consider the dynamical system (8). The stability boundary of its SEP is the boundary of the basin of attraction (BOA), which can be estimated based on the following observation: if the system trajectory starting from an initial state converges to the SEP, that initial state is inside the BOA; otherwise, it is outside. The stability boundary can be numerically identified by the search algorithm below, similar to the one in [20].

Step 1: In the w_{2i-1}-w_{2i} plane, set up M unit vectors with angles (in degree) respectively taking 0, 360/M, …, 360 (M-1)/M, say $\boldsymbol{n}_1$, …, $\boldsymbol{n}_M$. M = 180 is used in all studied cases in this paper.
Step 2: Set s to be a small step, e.g., 0.1 used in this paper. Along the direction determined by each of the unit vectors, say $\boldsymbol{n}_j$, let $\boldsymbol{w}_0$=$s\boldsymbol{n}_j$ and perform the steps 3-6 below.
Step 3: Use $\boldsymbol{w}_0 = s\boldsymbol{n}_j$ as the initial state to numerically solve (8) over a period of time (5 seconds in this paper) for $w_{2i-1}(t)$ and $w_{2i}(t)$.
Step 4: If $s < \varepsilon$, stop the search and $\boldsymbol{w}_0$ is an estimate of the boundary in direction $\boldsymbol{n}_j$; otherwise, go to step 5. ε in this stopping criterion defines the error tolerance which takes 0.01 in this paper.
Step 5: If the gap between the maximum and minimum of $w_{2i}(t)$ is >750°, let $\boldsymbol{w}_0 = \boldsymbol{w}_0 - s\boldsymbol{n}_j$ and $s = s/2$; otherwise, directly go to step 6.
Step 6: let $\boldsymbol{w}_0 = \boldsymbol{w}_0 + s\boldsymbol{n}_j$ and go to step 3.

This numerical search algorithm can give a fairly accurate estimate when step s and tolerance ε take very small values. The entire time cost is moderate since the system (8) only has two state variables. With this estimated boundary as a reference, the following will present two analytical approaches for estimating the stability boundary.

B. First integral

Eq. (9) gives a necessary and sufficient condition for (1) to have a first-integral based Lyapunov function. Unfortunately, there are no general methods for constructing a first-integral based Lyapunov function for nonlinear dynamical systems [19].

$$\sum_{j=1}^{N} \frac{\partial f_j}{\partial x_j} = 0 \tag{9}$$

With the help of NMD, after admitting the assumptions in (10) and (11), the system in (8) can be transformed to (12), and a Lyapunov function $V(w_{2i-1},w_{2i})$ for (8) can be constructed as in (13) by (9).

$$\begin{cases} \upsilon_{ijl} = 0 & \text{for all } j \ge 1, l \ge 1, j + l \le k, (j,l) \ne (1,0) \\ \nu_{ijl} = 0 & \text{for all } j \ge 0, l \ge 0, 2 \le j + l \le k \end{cases} \tag{10}$$

$$\upsilon_{i10} = 0 \tag{11}$$

$$\begin{cases} w_{2i-1} = \sum_{l=1}^{k} \upsilon_{i0l} w_{2i}^{l} \\ w_{2i} = w_{2i-1} \end{cases} \tag{12}$$

$$\frac{dw_{2i}}{dw_{2i-1}} = \frac{w_{2i}}{w_{2i-1}} = \frac{w_{2i-1}}{\sum_{j=1}^{k} \upsilon_{ij} w_{2i}^{j}} \Rightarrow V(w_{2i-1}, w_{2i}) \tag{13}$$
$$= \frac{w_{2i-1}^2}{2} - \int_0^{w_{2i}} \sum_{j=1}^{k} \upsilon_{ij} s^j \, ds = \frac{w_{2i-1}^2}{2} - \sum_{j=1}^{k} \frac{\upsilon_{ij}}{j+1} w_{2i}^{j+1}$$

Note that the assumption in (10) changes the nonlinear characteristics of the system, while the assumption (11) forces the oscillation damping to zero, which does not have a significant influence on the stability analysis result. Validated by the numerical studies presented later in subsections V-B and V-C, the coefficients ignored by (10) are always found to be small and ignoring positive damping can keep the stability analysis based on (12) to be conservative.

For each decoupled system in (12), the closest UEPs denoted by $w_{2i,\mathrm{UEP}}$ can be obtained by letting the right hand side be zero and solving the resulting algebraic equations for the roots with the smallest magnitude. Note that there may be one or two (a positive one and a negative one) closest UEPs depending on the order k. Then, the critical energy is defined as $V(0, w^*_{2i})$, where w^*_{2i} is selected as the UEP having a smaller energy. When the systems in (12) has an initial state $(w_{2i-1}(0), w_{2i}(0))$, it is stable if and only if $V(0, w^*_{2i}) \geq V(w_{2i-1}(0), w_{2i}(0))$. Therefore, the stability boundary of (8) can be approximated by an equipotential curve of (12) with the potential of $V(0, w^*_{2i})$, i.e.:

$$V(w_{2i-1}, w_{2i}) = V(0, w^*_{2i}) \tag{14}$$

C. Zubov's method

A Lyapunov function $V(\mathbf{x})$ for determining the exact stability boundary of the ordinary differential equations in (1) can be constructed by solving the partial differential equation in (15), called the Zubov's equation [21][22]. Note that the mode-decoupled system in (8) is a special case of the general system in (1). Thus, this subsection only applies the Zubov's method to (1). All conclusions drawn are automatically applicable to (8).

$$\sum_{j=1}^{N} \frac{\partial V(\mathbf{x})}{\partial x_j} f_j(\mathbf{x}) = -\varphi(\mathbf{x}) \cdot \left(1 - V(\mathbf{x})\right) \tag{15}$$

where $\varphi(\mathbf{x})$ is a positive definite or semidefinite function of $\mathbf{x}$. Note that $\varphi(\mathbf{x})$ must be chosen before solving the above equation, and its selection will not influence the resulting stability boundary.

Several necessary theorems (see proofs in [21]) and definitions are briefly reviewed below due to their importance for understanding the Zubov's method based stability analysis.

Theorem III-C1. The function $V(\mathbf{x})$ solved from (15) is a Lyapunov function establishing the asymptotic stability of the unperturbed motion at the SEP of the system (1).

Definition III-C1. Let Ω be the set of the initial values $\mathbf{x}_0$ which make up the domain of asymptotic stability of the unperturbed motion at the SEP of the system in (1). Thus, Ω is the BOA of the system (1).

Theorem III-C2. If $\mathbf{x}$ is in Ω, then

$$0 \leq V(\mathbf{x}) < 1 \tag{16}$$

Theorem III-C3. The stability boundary of the system in (1), i.e. the boundary of Ω, is the surface defined by $V(\mathbf{x}) = 1$.

Eq. (15) has a closed-form solution only for very special cases, while the solution of a general case can always be represented in a power series form (17), where $V_j(\mathbf{x})$ represents all homogeneous terms of order j in $\mathbf{x}$. Truncating the terms above order L, an approximate of $V(\mathbf{x})$ is given in (18).

$$V(\mathbf{x}) = \sum_{j=2}^{\infty} V_j(\mathbf{x}) \tag{17}$$

$$V(\mathbf{x}) \approx V^{(L)}(\mathbf{x}) = \sum_{j=2}^{L} V_j(\mathbf{x}) \tag{18}$$

Definition III-C2. Given $V^{(L)}(\mathbf{x})$ in (18), define the set Φ and the constant scalar $v^{(L)}$ respectively by (19) and (20).

$$\Phi = \{\mathbf{x} \mid \dot{V}^{(L)}(\mathbf{x}) = 0\} \tag{19}$$

$$v^{(L)} = \min\{V^{(L)}(\mathbf{x}) \mid \mathbf{x} \in \Phi\} \tag{20}$$

Theorem III-C4. The surface $V^{(L)}(\mathbf{x}) = v^{(L)}$ is completely contained in Ω.

Remark: Note that even though there is no theoretical difficulty in estimating the stability boundary from (19)-(20), there could be a huge computational burden for systems with high dimensions [23]. Thus, the above analysis is applied to each of the mode-decoupled systems in (8) rather than the original N-dimensional system in (1). In theory, the Lyapunov function with infinite terms in (17) is independent of the choice of the function φ used in the Zubov's equation (15). However, when a finite number of terms are kept in (18), the choice of the function φ influences the rate of convergence. In addition, the intuition that keeping more terms will always give better accuracy is unnecessarily true even for an SMIB system [24]. The optimal selection of the function and the order L is not a focus of this paper but deserves further investigations [25]. In the rest of this paper, we choose φ and L based on our experience on extensive case studies and use them for all test cases.

IV. Nonlinear Modal Decoupling Based Power System Transient Stability Analysis

Although there are no theoretical limitations in applying the nonlinear modal decoupling to any sizes of multi-machine power systems, the computational burden will be a limiting factor for large-scale power systems. This section first presents the direct application of NMD based transient stability analysis (TSA) for small-scale multi-machine power systems, and then introduces an idea on extending such analysis to large-scale power systems.

A. Power system modeling

Consider an m-machine power system in the classical model, whose generators are represented by the second-order swing equation and loads by constant impedances:

$$\ddot{\delta}_i + \frac{\varsigma_i}{M_i}\dot{\delta}_i + \frac{\omega_s}{M_i}\left(P_{mi} - P_{ei}\right) = 0 \tag{21}$$

$$P_{ei} = E_i^2 g_i + \sum_{j=1, j\neq i}^{m}\left[a_{ij}\sin(\delta_i - \delta_j) + b_{ij}\cos(\delta_i - \delta_j)\right] \tag{22}$$

where $i \in \{1,2,\ldots,m\}$, δ_i, P_{mi}, P_{ei}, E_i, M_i and ς_i respectively represent the absolute rotor angle, mechanical power, electrical power, electromotive force, inertia constant and damping constant of machine i, and g_i, a_{ij}, and b_{ij} represent network parameters including all loads.

Assume that the system has a uniform damping, i.e. $\varsigma_i/M_i=\varsigma_j/M_j$ for any i,j. It has been shown that (i) the oscillatory dynamics and the stability of the system are dominated by the relative motions among different machines [26][27]; and (ii) those relative motions can always be represented by an (m-1)-oscillator system [28].

Denote $\hat{\mathbf{x}}=[\boldsymbol{\delta}^T\ \dot{\boldsymbol{\delta}}^T]^T$ as the state vector. Then, the first-order differential equaitons of the system in (21)-(22) have the form

$$\dot{\hat{\mathbf{x}}} = \mathbf{f}_0(\hat{\mathbf{x}}) \tag{23}$$

Apply a transformation matrix R, whose columns are right eigenvectors of $\mathbf{f}_0$'s Jacobian matrix, to both sides of (23) to obtain its modal space representation in (24), where $\mathbf{y}=[y_1\ y_2\ \ldots\ y_{2m}]^T$ is the new state vector.

$$\dot{\mathbf{y}} = R^{-1}\mathbf{f}_0(R\mathbf{y}) \triangleq \mathbf{g}(\mathbf{y}), \quad \text{where } \mathbf{y} = R^{-1}\hat{\mathbf{x}} \tag{24}$$

Without loss of generality, let y_1, y_2, ..., y_{2m-2} represent the relative motions of the system, and y_{2m-1} and y_{2m} represent the mean motions, which are non-oscillatory dynamics that all generators are moving together. It has been proved in [28] that the relative motions can be represented by an (m-1)-oscillator system consisting of different equations about y_1, y_2, ..., y_{2m-2}. Thus, the first (2m–2) equations of (24) are the model in (1) with N = (2m–2), to which the NMD will be applied.

B. NMD based TSA for small multi-machine power systems

For a power system with not-many machines, the NMD can be applied directly to the entire system to determine (m–1) independent second-order systems in the form of (8) with polynomial nonlinearities up to a desired order k, as shown by the following procedure (named "**NMD-TSA 1**"):

Step 1: Given an m-machine system represented by (23), derive the modal space representation (24).
Step 2: Assume uniform damping and obtain a unique (m–1)-oscillator system by the first (2m–2) equations in (24).
Step 3: Apply NMD to this (m–1)-oscillator system to obtain (m–1) decoupled second-order systems in the form of (8) that respectively correspond to (m–1) oscillatory modes.
Step 4: Apply a stability analysis in Section III to estimate the stability boundary of each of these (m–1) nonlinear oscillators.
Step 5: For the original system, i.e. (24) or (21)-(22), given any trajectory subjected to a disturbance of interest, transform it to the decoupled coordinates using transformations (2) and (7), and visualize the transformed trajectory. If the trajectory does not exceed the stability boundary obtained in step 4 for any mode, the system subject to that disturbance is assessed to be stable; otherwise, it is considered unstable.

The stability boundary of each mode-decoupled system actually represents a portion of the stability boundary of the original system that is projected to the decoupled coordinates about one mode.

C. NMD based TSA for large multi-machine power systems

For a large-scale multi-machine power system, the above **NMD-TSA 1** could be computationally expensive. It is often observed that when a power system is subject to a disturbance, usually only a few modes are significantly excited while the rest of the modes are either quiescent or less influential in stability of the system. Thus, a large-scale system can be reduced to a smaller system only about the dynamics associated with those few selected modes.

Re-write the first (2m–2) equations in (24) as (25), which partitions (2m–2) equations into two groups: one group for the modes of interest (denoted with subscript "int") and the other group for the rest of modes (denoted with subscript "non").

$$\begin{pmatrix}\dot{\mathbf{y}}_{int}\\ \dot{\mathbf{y}}_{non}\end{pmatrix} = \begin{pmatrix}\mathbf{g}_{int}(\mathbf{y}_{int},\mathbf{y}_{non})\\ \mathbf{g}_{non}(\mathbf{y}_{int},\mathbf{y}_{non})\end{pmatrix} \tag{25}$$

Ignore the dynamics with the second group, i.e. admitting (26). Then, eq. (25) is reduced to (27) containing only the modes of interest.

$$\begin{cases}\mathbf{y}_{non} = \mathbf{0}\\ \mathbf{y}_{non} = \mathbf{0}\end{cases} \tag{26}$$

$$\dot{\mathbf{y}}_{int} = \mathbf{g}_{int}(\mathbf{y}_{int}, \mathbf{0}) \tag{27}$$

Then, apply NMD to (27) and perform a stability analysis on each of the resulting mode-decoupled systems to obtain TSA results. The above enhanced TSA procedure for large-scale multi-machine systems is named "**NMD-TSA 2a**".

Remarks:

- In this paper, we called a multi-machine power system small or large mainly depending on computational requirement of the proposed approach. Currently, the derivation of NMD is implemented using Symbolic Math Toolbox in Matlab, which is not highly efficient. Thus, power systems with 2-6 machines are thereby called small systems, while those with more machines are called large systems. Since NMD has similar computation procedures to normal form [14]-[16], a more efficient implementation is also achievable, with which power systems with up to 50 machines may be considered as small [29].
- In addition, The **NMD-TSA 2a** procedure may introduce errors to TSA in two aspects. First, to reduce the large-scale system, dynamics with most modes that having little impact on stability are neglected, and hence the stability boundary estimated with respect to the modes of interest may not exactly match the true boundary. Second, inter-modal terms of orders >k are not considered in the decoupled systems but they may become unneglectable

when the system state is far from the SEP, especially when approaching the transient stability boundary. Therefore, even if **NMD-TSA 2a** judges a post-disturbance trajectory to be stable, there is still a possibility that the original system may exit the true stability boundary due to influences from the ignored modes and high order inter-modal terms.

To address the issue in the second remark, a shrinking ratio r defined in (28) is adopted to shrink the stability boundary about the ith mode in (27) based on estimates of modal energies by (29)-(31). Here, we assume that the speed deviation of any generator rotor can be represented by a sum of sinusoids as shown in (31) about excited modes in (27). The representation (31) can be estimated by modal analysis tools, e.g. Prony and Matrix pencil methods, on stable trajectories.

$$r_i \overset{\Delta}{=} E_i / E_{\text{all}} \tag{28}$$

$$E_i \overset{\Delta}{=} a\sum\nolimits_{j=1}^{m} H_j A_{ji}^2 \tag{29}$$

$$E_{\text{all}} \overset{\Delta}{=} \sum\nolimits_i E_i \tag{30}$$

$$\Delta\omega_j(t) = A_{ji}e^{\sigma_i t}\cos(\Omega_i t + \phi_{ji}) + \sum\nolimits_{k\neq i} A_{jk}e^{\sigma_k t}\cos(\Omega_k t + \phi_{jk}) \tag{31}$$

where E_i and E_{all} respectively represents the transient energies of mode i and all modes; H_j is the inertia constant of machine j; a is a certain constant, whose value does not affect the shrinking ratio r_i at all; $\Delta\omega_j(t)$ represents the trajectory of speed deviation of machine j, with A_{jk}, ϕ_{jk}, σ_{jk} and Ω_k as the amplitude, phase, damping and frequency of mode k.

The procedure that additionally applies the shrinking ratio to the stability boundary about each mode is named "**NMD-TSA 2b"** for comparison purposes. For instance, the estimated stability boundaries by the aforementioned first integral method and the Zubov's method become $V(w_{2i\text{-}1}, w_{2i}) = r_i V(0, w^*_{2i})$ and $V^{(L)}(\mathbf{x}) = r_i v^{(L)}$, respectively. Note that calculation of the shrinking ratio requires a stable trajectory and is contingency-dependent, while **NMD-TSA 1** and **2a** are contingency-independent.

To summarize, NMD-based TSA for general power systems may contain three types of error: (i) truncation errors due to ignoring high-order Taylor expansion terms of (1), (ii) model decoupling errors due to ignoring inter-modal terms of orders $>k$ of (2), and (iii) the estimation errors of the stability boundary. Ref. [18] investigated the first type of errors and suggests that a third order polynomial truncation be used for both conservative stability assessment and moderate computational burden, which will be adopted in case studies.

V. Case Studies

The first test is performed on an SMIB power system to investigate the third type of errors by comparing the stability boundaries estimated by the first integral method and Zubov's method to the reference result calculated by time simulations. The second test is on the 9-bus power system and investigates the second type of errors by comparing the three procedures: **NMD-TSA 1**, **2a** and **2b**. The third test is conducted on a simplified NPCC 140-bus power system to show the potential application of the NMD based TSA for early warning of the oscillatory mode that may most likely develop into a transient instability in a large 48-machine 140-bus NPCC power system. Finally, to test to what extent the NMD based TSA, which is based on classical model, can work for the power systems with detailed generator model, the detailed NPCC 140-bus power system is simulated with the same contingency in the third test, and visualize the marginal stable and unstable trajectories in the decoupled systems determined by the classical model.

A. Test on an SMIB system

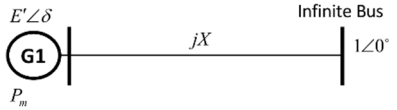

Fig.1. An SMIB power system

Consider a general SMIB power system whose swing equation is shown in (32) [30].

$$\begin{cases} \dot{\delta} = \omega \\ \dot{\omega} = \dfrac{P_{\max}\omega_{\text{s}}}{2H}\left(\sin\delta_{\text{s}} - \sin(\delta+\delta_{\text{s}})\right) - \dfrac{D}{2H}\omega \end{cases} \tag{32}$$

where δ and ω are respectively the relative rotor angle about its steady state value δ_{s} and speed deviation, ω_{s} is the synchronous angular speed, D and H are the damping and inertia constants, respectively, and $P_{\max}$ is the maximum power transfer. Let parameters take the following values [31]: δ_{s}= 15°, ω_{s}= 2π×60 rad/s, D=1, H=3s, $P_{\max}$=1.7 p.u..

The third-order polynomial approximate of (32) at the origin (the SEP) is shown below.

$$\begin{cases} \dot{\delta} = \omega \\ \dot{\omega} = -0.1667\omega - 103.2\delta + 13.82\delta^2 + 17.2\delta^3 \end{cases} \tag{33}$$

Using the first integral method with the assumptions in (10) and (11), the system (33) is reduced to (34) and the resulting Lyapunov function is (35).

$$\begin{cases} \dot{\delta} = \omega \\ \dot{\omega} = -103.2\delta + 13.82\delta^2 + 17.2\delta^3 \end{cases} \tag{34}$$

$$V(\omega,\delta) = 0.5\omega^2 + 51.59\delta^2 - 4.608\delta^3 - 4.299\delta^4 \tag{35}$$

The two closest UEPs are δ_{uep1} = 2.0803rad and δ_{uep2} = –2.8842rad with energies $V(0,\delta_{\text{uep1}})$ = 101.3 and $V(0,\delta_{\text{uep2}})$ = 242.2. Thus, $V(0,\delta_{\text{uep1}})$ is defined as the critical energy and the corresponding stability boundary is estimated as (36).

$$0.5\omega^2 + 51.59\delta^2 - 4.608\delta^3 - 4.299\delta^4 = 101.3 \tag{36}$$

In the Zubov's method based approach, choose $\varphi(\omega,\delta)$ as

$$\varphi(\omega,\delta) = 0.0002\omega^2 + 0.001\delta^2 \tag{37}$$

Let L=16, which is adopted in all case studies with Zubov's method. Due to the size of the solution for L=16, we only illustrate the resulting Lyapunov function for L=5, i.e. $V^{(5)}$:

$$
\begin{aligned}
V^{(5)}(\omega,\delta) &= 6.291\times10^{-4}\omega^2 + 9.692\times10^{-6}\omega\delta + 0.06491\delta^2 \\
&+8.386\times10^{-9}\omega^3 + 4.193\times10^{-9}\omega^2\delta + 1.299\times10^{-6}\omega\delta^2 \\
&-5.797\times10^{-3}\delta^3 - 1.771\times10^{-7}\omega^4 + 7.75\times10^{-9}\omega^3\delta \\
&-3.654\times10^{-5}\omega^2\delta^2 + 1.16\times10^{-6}\omega\delta^3 - 7.294\times10^{-3}\delta^4 \\
&+3.172\times10^{-11}\omega^5 + 2.811\times10^{-11}\omega^4\delta + 8.192\times10^{-9}\omega^3\delta^2 \\
&+3.269\times10^{-6}\omega^2\delta^3 + 4.281\times10^{-7}\omega\delta^4 + 3.369\times10^{-4}\delta^5
\end{aligned} \tag{38}
$$

All following calculations are based on $V^{(16)}$. The critical energy in (20) is found to be $v^{(16)} = 0.1142$ and the stability boundary is estimated as (39).

$$V^{(16)}(\omega,\delta) = v^{(16)} = 0.1142 \tag{39}$$

The stability boundaries of the system (33) determined by first integral, Zubov's method and time simulations are compared in Fig.2, which shows that the boundaries by first integral and Zubov's method are completely inside and fairly close to that by time simulations. Fig.2 also compares the stability boundaries of (33) and (32) by time simulations and shows that the third-order truncation in (33) consistently gives conservative stability analysis results for the system in (32).

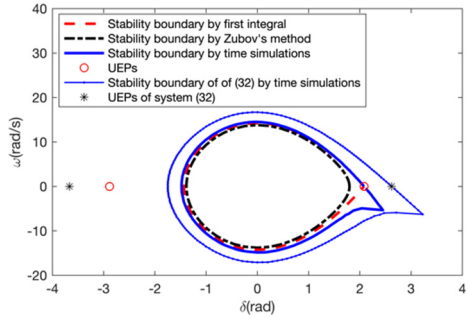

Fig.2. Stability boundaries estimated by different approaches.

B. Test on a 3-machine 9-bus power system

Consider the 3-machine, 9-bus system [32] in the classical model [33], whose one-line diagram and the system equations corresponding to (23), (24), (5) and (8) after the studied contingency in this paper can be found as Fig.2, equations (56), (57), (59) and (61) in ref. [11]. Consider a temporary three-phase fault at bus 5 with the line 5-7 tripped upon the clearance of the fault, and the TSA is performed for the post-contingency system. The post-contingency system has two electromechanical modes, i.e. 0.96Hz and 2.05Hz, such that we have two mode-decoupled systems in the form of (8).

First, we apply **NMD-TSA 1** to analyze the two mode-decoupled systems. Fig.3(a) and Fig.3(b) show the identified stability boundaries by first integral, Zubov's method and time simulations (legends are the same as Fig.2), where a marginally stable trajectory with fault cleared after 8 cycles and a marginally unstable trajectory with fault cleared after 9 cycles are also drawn. Comparing Fig.3(a) and Fig.3(b) we can see that under this contingency, the 0.96Hz mode would more likely develop into an instability under such a large disturbance, while the 2.05Hz mode is quite stable and only exhibits small dynamics even when the system becomes unstable. For each of the two modes, the BOA from Zubov's method is completely contained by that from time simulations, which means Zubov's method consistently provides conservative stability analysis results. However, a small portion of the BOA from the first integral method is outside of that from time simulations, which indicates that the first integral method may fail to identify some unstable cases. The time domain results of the two marginal cases are provided in Fig.4, whose projections in the two mode-decoupled coordinates in Fig.3(a) and Fig.3(b) can be clearly differentiated by the NMD based stability analysis, confirming the accuracy of the **NMD-TSA 1**.

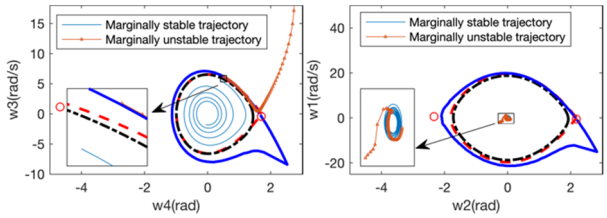

(a) 0.96Hz (b) 2.05Hz

Fig.3. Stability boundaries of mode-decoupled systems by NMD-TSA 1.

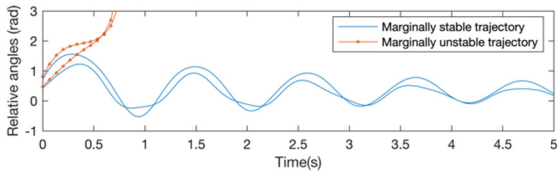

Fig.4. Marginally stable and unstable relative angles w.r.t. generator 1.

To validate **NMD-TSA 2a**, the simplified modal representation in the form of (27) is formulated for the 0.96Hz mode only, since the system dynamics seem to be dominated by this mode. The simplified formulation is then used to identify the stability boundary as shown in Fig.5(a), which is almost the same as Fig.3(a). This implies that ignoring the dynamics with the 2.05Hz mode does not introduce significant errors to the stability analysis on the 0.96Hz mode in this test. Such a simplification is also valid for stability analysis on the 2.05Hz mode with the dominant 0.96Hz mode ignored as shown in Fig.5(b).

In addition, the two modes can be selected simultaneously to be analyzed by NMD-TSA 2a. In this case, **NMD-TSA 2a** is the same as **NMD-TSA 1**.

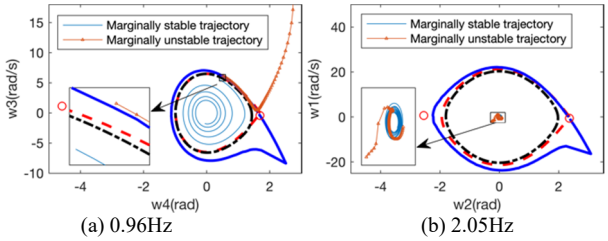

(a) 0.96Hz (b) 2.05Hz

Fig.5. Stability boundaries of mode-decoupled systems by NMD-TSA 2a.

To check the performance of **NMD-TSA 2b**, we first apply NMD to both modes. Then, the marginally stable trajectory is adopted to calculate the shrinking ratio for each mode, which is then used to determine the shrunk BOAs by first integral and Zubov's method. The results are shown in Fig.6(a) and Fig.6(b) with r_1=0.914 and r_2=0.086, respectively. Comparing Fig.6(a) to Fig.3(a) or Fig.5(a), the estimated stability boundary for the dominant 0.96Hz mode is slightly changed. From Fig.6(b), the BOA for the 2.05Hz mode is significantly shrunk. As expected, more conservative stability analysis is resulted. Under this studied contingency, it is obvious that the

system is quite stable with the 2.05Hz mode and is more likely to lose stability with the 0.96Hz mode.

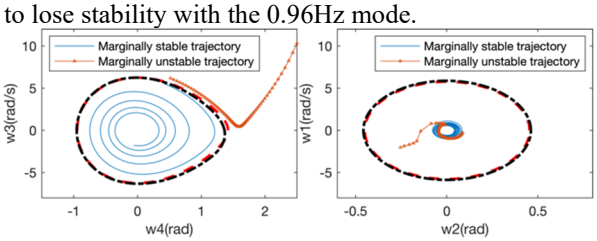

(a) 0.96Hz (b) 2.05Hz

Fig.6. Stability boundaries of mode-decoupled systems by NMD-TSA 2b.

C. Test on NPCC 140-bus power system with classical model

The third test is performed to demonstrate a potential application of NMD based TSA for early warning of the oscillatory mode that may most likely develop into a transient instability in large power systems. A simplified NPCC system is adopted for this purpose [34][35], which contains 48 generators and 140 buses. A temporary three-phase fault is added at bus 13 and cleared after a certain time without disconnecting any line. The critical clearing time of this contingency is 0.16 second and the resulting post-contingency response is shown in Fig.7. By calculating the modal energies according to the definition in (29)-(31), it is found that this fault only largely excites a few modes, as indicated by Table I. When the fault duration increases to 0.17s, the system will lose its stability as shown in Fig.8, where all rotor angles are divided into two clusters. The diagram of NPCC 140-bus system and the two clusters are shown in Fig. 8.

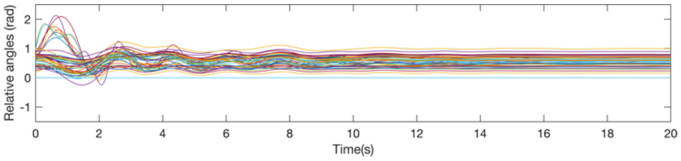

Fig.7. Marginally stable relative rotor angles w.r.t. generator 78.

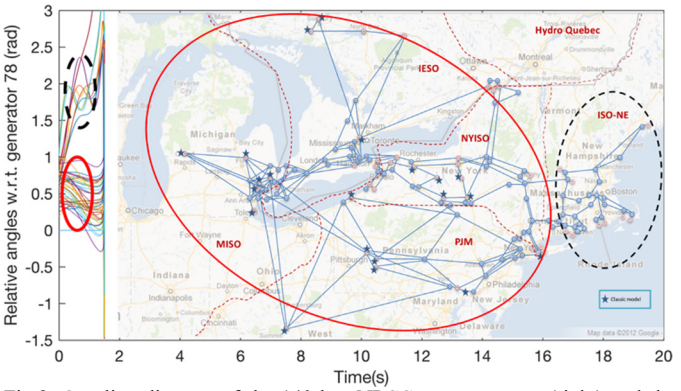

Fig.8. One-line diagram of the 140-bus NPCC power system (right) and the marginally unstable relative rotor angles w.r.t. generator 78 (left).

The **NMD-TSA 2b** is applied to the top-five largely excited modes. The stability boundaries estimated by **NMD-TSA 2b** with first integral and Zubov's method about five modes are shown in Fig.9, respectively. The legends are the same as those in Fig.2 and Fig.6. On one hand, it should be noted that the complex behaviors of generators shown in Fig.7 become much simpler to understand in Fig.9, which clearly shows whether the system is going back to the SEP or not upon the fault clearance. When the marginally stable contingency occurs, the 0.6Hz mode in Fig.9(d) is more likely to transit to instability modes because the post-contingency state of the system is close to the boundary. Thus, an early warning signal should be generated to request for preventive control actions. On the other hand, the four modes in Fig.9(a)(b)(c)(e) are quite stable even though they are excited to exhibit noticeable dynamics. In addition, note that the two split clusters of generators under the marginally unstable contingency match the mode shape of the 0.6Hz mode, which further validates the correctness of the early warning produced by the proposed method.

TABLE I
MODAL ENERGY UNDER THE STUDIED CONTINGENCY

f_i(Hz)	E_i^*	f_i(Hz)	E_i	f_i(Hz)	E_i	f_i(Hz)	E_i
0.38	**1**	1.28	$<10^{-3}$	1.57	$<10^{-4}$	1.69	$<10^{-6}$
0.26	**0.51**	1.56	$<10^{-3}$	1.58	$<10^{-5}$	1.99	$<10^{-6}$
0.53	**0.17**	0.96	$<10^{-3}$	1.40	$<10^{-5}$	1.45	$<10^{-6}$
0.60	**0.12**	1.04	$<10^{-3}$	1.68	$<10^{-5}$	2.51	$<10^{-6}$
0.47	**0.02**	0.83	$<10^{-3}$	1.28	$<10^{-5}$	1.70	$<10^{-7}$
2.44	0.01	0.95	$<10^{-3}$	1.20	$<10^{-5}$	1.41	$<10^{-7}$
1.27	$<10^{-2}$	0.91	$<10^{-3}$	1.63	$<10^{-5}$	1.51	$<10^{-8}$
1.14	$<10^{-2}$	1.55	$<10^{-3}$	2.14	$<10^{-5}$	1.87	$<10^{-8}$
1.41	$<10^{-2}$	1.38	$<10^{-4}$	2.09	$<10^{-5}$	1.85	$<10^{-9}$
0.72	$<10^{-2}$	1.78	$<10^{-4}$	1.33	$<10^{-6}$	1.69	$<10^{-10}$
0.70	$<10^{-3}$	1.72	$<10^{-4}$	2.06	$<10^{-6}$	1.35	$<10^{-33}$
1.08	$<10^{-3}$	1.17	$<10^{-4}$	1.78	$<10^{-6}$		

* All the model energies are normalized by the energy of the 0.38Hz mode

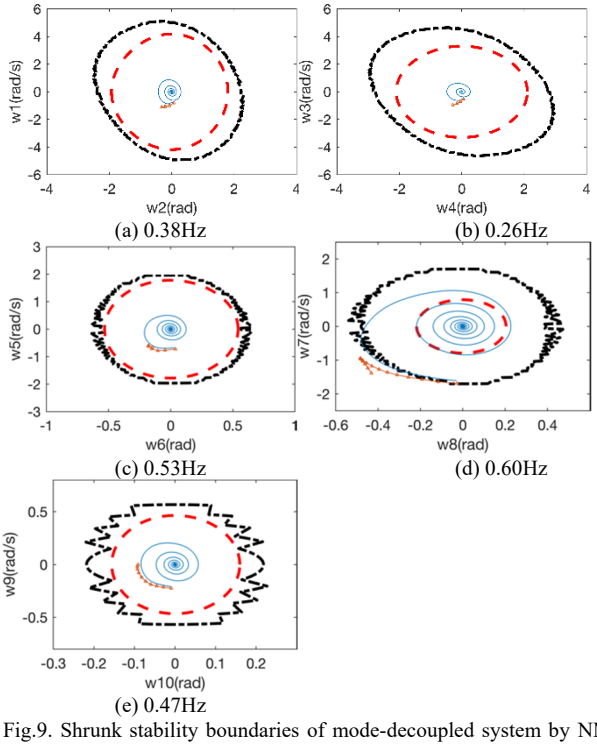

(a) 0.38Hz (b) 0.26Hz (c) 0.53Hz (d) 0.60Hz (e) 0.47Hz

Fig.9. Shrunk stability boundaries of mode-decoupled system by NMD-TSA 2b. Trajectories are obtained using classical model.

Therefore, mode-by-mode stability information can be assessed by the NMD based TSA to signal an early warning of the oscillatory mode that may most likely develop into a transient instability in a large power system. This information would be valuable for identification of the most vulnerable grid interface(s) for preventive/remedial control actions. However, by no means the proposed approach can replace the conventional simulation-based TSA tools since the results

from NMD based TSA are still approximate, as illustrated in Fig.9(d), where the marginally stable trajectory has a small portion located outside the BOA while the marginally unstable trajectory has a small portion inside.

The early warning provided by the NMD methodology is promising to be used in an out-of-step (OOS) protection system. The following strategy is one idea but will need further investigation. A nonlinear oscillator about the 0.6Hz mode, as shown in Fig. 9(d) by the proposed approach, can be embedded in a properly selected OOS relay, e.g. on the two interties connecting the regions of ISO New England and New York ISO. Multiple variations of the oscillator can be prepared offline representing different operating conditions. In the online environment, measured system trajectory (assuming the availability of wide-area measurement data) can be transformed into the coordinates regarding the 0.6Hz oscillator for prediction of OOS between the two regions. Such a strategy may coordinate with traditional OOS logics to enable a more adaptive special protection system.

D. Test on NPCC 140-bus power system with detailed models

The purpose of the fourth test is to show to what extent the NMD based TSA result based on the classical model can work for the stability analysis with the associated detailed model. The detailed NPCC 140-bus power system with excitation and governor controls [35] is simulated with the same contingency in Section V-C.

The projection of the marginally stable and unstable trajectories to each mode are shown in Fig. 10, whose legends are the same as those in Fig.2 and Fig.6. Comparing Fig. 10 to Fig. 9, it is observed that the difference compared to the trajectories from the associated classical model seems not significant in the decoupled coordinates. Therefore, the modeling details of the generator do not affect the overall accuracy, which implies that the major error in the entire process of NMD is from the two truncations, i.e. truncating Taylor expansion and truncating high-order nonlinear terms in the decoupled system, such that the modeling error seems to be buried by the truncation errors and would be difficult to be distinguished from the overall error. A reasonable work plan would be to first evaluate and reduce the impact of the truncation error, which is our ongoing work (some preliminary result is provided by [13]), and then investigate the impact from using a simplified generator model.

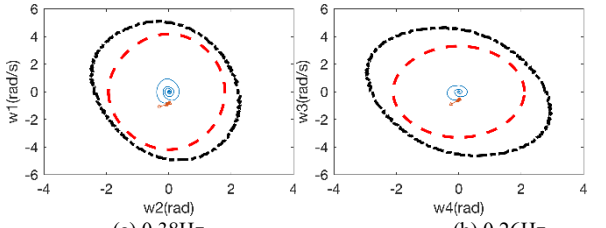

(a) 0.38Hz (b) 0.26Hz (c) 0.53Hz (d) 0.60Hz

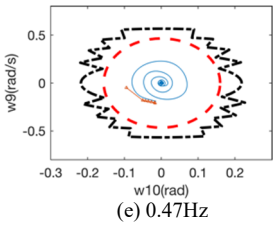

(e) 0.47Hz

Fig.10. Shrunk stability boundaries of mode-decoupled system by NMD-TSA 2b using classical model. Trajectories are obtained using detailed model.

E. Computational complexity and scalability

All tests presented in this section are performed in Maltab on an Intel Core i5 2.6GHz laptop computer. The offline derivation is implemented using Symbolic Math Toolbox in Matlab and the overall time cost for deriving the NMD transformations and mode-decoupled systems is listed in Table II. Due to the similarity in the calculation between the conventional normal form [14]-[16] and the proposed NMD, a more efficient implementation of NMD seems possible and would be able to deal with power systems with up to 50 machines (without any model reduction) within a tractable time [29]. It is also worth mentioning that in most cases of realistic large-scale power systems, only few modes, e.g. six or fewer modes [17], are largely excited even by a severe contingency. Therefore, the NMD has potential applications to a realistic large power system especially when the dynamics regarding few modes of the system are of interest. These possibilities can be explored in detail as future work.

TABLE II
TIME COSTS FOR DERIVING 3RD-ORDER NONLINEAR MODAL DECOUPLING

Systems	Dimensions of associated oscillator systems	Elapsed CPU Time
IEEE 9-bus system	4	7.04 sec
NPCC 140-bus system	10	2587 sec

NMD can always be calculated offline, e.g. every 15-30 minutes, and used in real time. In the online environment, one only needs to transform a few actual system states from, e.g., measurements or other faster-than-real-time simulations to the decoupled coordinates for transient stability assessment and visualization. In the online computation, converting all points of an unstable trajectory could be time-consuming and unnecessary, e.g. converting all 426 points of the unstable trajectory in Fig. 8 takes about 16s in Matlab to get the red curve in Fig. 10(d). Instead, we only need to convert very few points if they can help identify the mode most likely developing into an instability. For instance, converting those selected 5 points on the unstable trajectory takes only less than 0.3s. In addition, the online time cost can be further reduced by ignoring low-impact states, e.g. with small participation factors w.r.t. the modes of interest, and small coefficients in the NMD transformations. Such a potential improvement will be investigated in future. As a comparison, a 5-second time-domain simulation performed for the same NPCC 140-bus system in Power System Toolbox [34] takes about 13 seconds. Thus, the proposed NMD based approach for early warning of oscillatory modes that may develop to an instability mode is promising for online application.

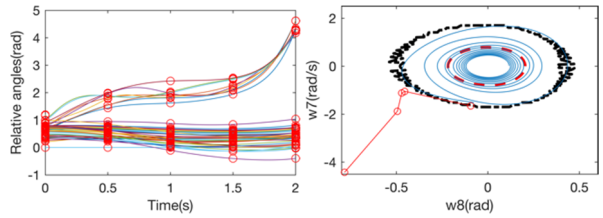

(a) Marginally unstable relative angles (b) 0.60Hz mode

Fig.11. Five selected state points (red circles).

VI. Conclusions and Future Work

For general multi-oscillator systems including multi-machine power systems in the classical model, the previously proposed nonlinear modal decoupling (NMD) approach provides an approximate representation for stability analysis, i.e. a number of decoupled nonlinear one-degree-of-freedom oscillators. This paper adopts the NMD approach and analyzes the transient stability of each of the decoupled nonlinear oscillators to infer the transient stability of the original multi-machine power systems by using the Lyapunov function theory. The proposed idea is validated on a single-machine-infinite-bus power system, the 9-bus power system, and the simplified and detailed NPCC 140-bus power system. Test results show that the NMD based analysis has a potential to assess the transient stability and visualize the modal dynamics of multi-machine power systems.

The potential significant benefits from NMD include: (i) a rough estimation of transient stability boundary; (ii) an early warning of the oscillatory mode that may most likely develop into a transient instability; (iii) visualization of the dynamics of a high-dimensional dynamical system in many low-dimensional coordinates for stability monitoring purpose. Future works will investigate in detail the online applications of the proposed NMD methodology, early warning of transient instability and out-of-step protection, using a more efficient implementation and also the design of preventive and remedial control actions. Comparisons to other tools [4][10] will also be performed.

VII. References

[1] NERC, "1996 System Disturbances – Review of Selected 1996 Electric System Disturbances in North America," Aug. 2002.

[2] U.S.-Canada Power System Outage Task Force, "Final Report on the August 14, 2003 Blackout in the United States and Canada: Causes and Recommendations," Apr. 2004.

[3] S. K. Khaitan, "A survey of high-performance computing approaches in power systems," *IEEE PES General Meeting*, Boston, 2016.

[4] V. Centeno, A. G. Phadke, A. Edris, J. Benton, M. Gaudi, and G. Michel, "An adaptive out-of-step relay for power system protection," *IEEE Trans. Power Del.*, vol. 12, no. 1, pp. 61-71, Jan. 1997.

[5] C. Liu, M. Su, S. Tsay, and Y. Wang, "Application of a novel fuzzy neural network to real-time transient stability swings prediction based on synchronized phasor measurements," *IEEE Trans. Power Syst.*, vol. 14, no. 2, pp. 685-692, May 1999.

[6] K. Sun, *et al*, "An online dynamic security assessment scheme using phasor measurements and decision trees," *IEEE Trans. Power Syst.*, vol. 22, no. 4, pp. 1935-1943, Nov. 2007.

[7] J. Yan, C. Liu and U. Vaidya, "A PMU-based monitoring scheme for rotor angle stability," *IEEE PES General Meeting*, San Diego, 2012.

[8] F. Bai, Y. Liu, Y. Liu, K. Sun, *et al*, "A measurement-based approach for power system instability early warning," Protection and Control of Modern Power Systems, 2016.

[9] I. B. Yadykin, *et al*, "Characterization of power systems near their stability boundary by Lyapunov direct method," *IFAC Proceedings Volumes*, vol.47, no.3, pp.9087-9092, 2014.

[10] K. R. Padiyar, *Structure Preserving Energy Functions in Power Systems: Theory and Applications*, CRC Press, 2016.

[11] B. Wang, K. Sun, W. Kang, "Nonlinear modal decoupling of multi-oscillator systems with applications to power systems," *IEEE Access*, vol.6, pp.9201-9217, 2018.

[12] X. Xu, B. Wang, K. Sun, "Approximation of closest unstable equilibrium points via nonlinear modal decoupling," *2019 IEEE PES General Meeting*, accepted.

[13] X. Xu, B. Wang, K. Sun, "Initial study of the power system stability boundary estimated from nonlinear modal decoupling," *2019 IEEE PES Powertech*, accepted.

[14] S. Wiggins, *Introduction to Applied Nonlinear Dynamical Systems and Chaos*. New York, NY, USA: Springer-Verlag, 1990.

[15] V. I. Arnold, *Geometrical Methods in the Theory of Ordinary Differential Equations*. New York, NY, USA: Springer-Verlag, 1988.

[16] V. Vittal, *et al*, "Analysis of stressed power systems using normal forms," *Proc. IEEE Int. Symp. Circuits Syst.*, San Diego, May 1992.

[17] IEEE Task Force on Identification of Electromechanical Modes, "Identification of electromechanical modes in power systems," *Technical Report PES-TR15 (formerly TP462)*, June 2012.

[18] B. Wang, X. Xu, K. Sun, "Power system transient stability analysis using high-order Taylor expansion systems," *Texas Power and Energy Conference*, College Station, 2019

[19] M. A. Pai, *Power System Stability*, New York: North-Holland Publishing Company, 1981.

[20] K. Sun, J. Qi, W. Kang, "Power system observability and dynamic state estimation for stability monitoring using synchrophasor measurements," *Control Engineering Practice*, vol. 53, pp. 160-172, 2016.

[21] V. I. Zubov, *Methods of A.M. Lyapunov and their application*, Izdatel'stvo Leningradskogo Universiteta, 1961.

[22] S. Margolis and W. Vogt, "Control engineering applications of V. I. Zubov's construction procedure for Lyapunov functions," *IEEE Trans. Autom. Control*, vol.8, no.2, pp. 104-113, Apr 1963.

[23] A. K. De Sarkar, N. D. Rao, "Zubov's method and transient stability problems of power systems," *Proc. IEE*, vol.118, no.8, pp.1035-1040, Aug. 1971.

[24] Y. Yu, K. Vongsuriya, "Nonlinear power system stability study by Liapunov function and Zubov's method," *IEEE Trans. Power App. Syst.*, vol.pas-86, no.12, pp.1480-1485, 1967.

[25] R. Genesio, M. Tartaglia, A. Vicino, "On the estimation of asymptotic stability regins: state of the art and new proposals," *IEEE Trans. Autom. Control*, vol.ac-30, no.8, pp.747-755, 1985.

[26] F. Saccomanno, "Electromechanical phenomena in a multimachine system," *Electric Power Systems*. New York: Wiley, 2003.

[27] P. Kundur et al., "Definition and classification of power system stability IEEE/CIGRE joint task force on stability terms and definitions," *IEEE Trans. Power Syst.*, vol. 19, no. 3, pp. 1387-1401, Aug. 2004.

[28] B. Wang, K. Sun, W. Kang, "Relative and mean motions of multi-machine power systems in classical model," *arXiv:1706.06226*, 2017.

[29] Z. Wang, Q. Huang, "A closed normal form solution under near-resonant modal interaction in power systems," IEEE Trans. on Power Syst., vol. 32, no. 6, pp. 4570-4578, Mar. 2017.

[30] B. Wang, K. Sun, A.D. Rosso, E. Farantatos, N. Bhatt, "A study on fluctuations in electromechanical oscillation frequency," *IEEE PES General Meeting*, National Harbor, 2014.

[31] B. Wang, K. Sun, "Formulation and characterization of power system electromechanical oscillations," *IEEE Trans. Power Syst.*, vol.31, no.6, pp.5082-5093, 2016.

[32] P. M. Anderson, *Power System Control and Stability*. Hoboken: Wiley IEEE Press, 2003.

[33] B. Wang, K. Sun, "Power system differential-algebraic equations," *arXiv:1512.05185*, 2015.

[34] J. Chow, G. Rogers, User manual for power system toolbox, version 3.0, 1991–2008.

[35] J. Qi, K. Sun, W. Kang, "Optimal PMU placement for power system dynamic state estimation by using empirical observability Gramian," *IEEE Trans. Power Syst.*, vol.30, no. 4, pp.2041-2054, 2015.

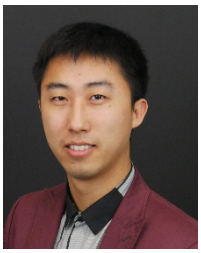

Bin Wang (S'14-M'18) received the B. S. and M.S. degrees from Xi'an Jiaotong University in 2011 and 2013, respectively, and Ph.D. degree from the University of Tennessee, Knoxville, all in Electrical Engineering. He is currently a postdoc researcher in the Department of Electrical and Computer Engineering at Texas A&M University. His research interests include power system dynamics, stability and control.

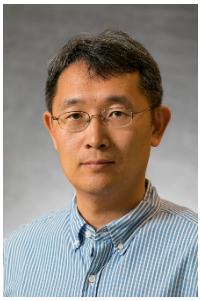

Kai Sun (M'06–SM'13) received the B.S. degree in automation in 1999 and the Ph.D. degree in control science and engineering in 2004 both from Tsinghua University, Beijing, China. He is an associate professor at the Department of EECS, University of Tennessee, Knoxville, USA. He was a project manager in grid operations and planning at the EPRI, Palo Alto, CA from 2007 to 2012. Dr. Sun serves in the editorial boards of IEEE Transactions on Power Systems, IEEE Transactions on Smart Grid and IEEE Access.

Xin Xu (S'15) received the B.E. and M.E. degree in electrical engineering from Shandong University, in 2013 and 2016, respectively. He is now pursuing his Ph.D. degree at the department of EECS, University of Tennessee at Knoxville. His main research interests include nonlinear system dynamics, stability assessment and control, and renewable resources.